PERGAMON

International Journal of Solids and Structures 37 (2000) 7703–7716

INTERNATIONAL JOURNAL OF SOLIDS and STRUCTURES

www.elsevier.com/locate/ijsolstr

2-D Normal compliances for elastic and visco-elastic binder contact with finite particle size effect

Han Zhu [a,*], Ching S. Chang [b], Ken A. Lou [c]

[a] *Civil and Environmental Engineering Department, Arizona State University, Tempe, AZ 85287-5306, USA*
[b] *Department of Civil and Environmental Engineering, University of Massachusetts, Amherst, MA 01003, USA*
[c] *Simula Technologies Inc., Phoenix, AZ 85044-5299, USA*

Received 10 June 1998; in revised form 18 November 1999

Abstract

The close-form 2-D normal force–displacement compliance relation (binder contact law) is derived for a system of two elastic cylindrical particles bound by an elastic or visco-elastic binder based on the approach developed by Zhu et al. (1996a,b, 1997b). A new result of finite particle size effect on the compliance is also obtained. One important application of this binder compliance is in the area of the homogenization analysis of fibrous composites, and computation of the binder compliance based effective transverse bulk modulus is conducted in this article with its comparison to the corresponding upper and lower bounds.

Keywords: Binder contact laws; Contact compliance; Visco-elastic binder; Displacement–force relation; Modulus and composites

1. Introduction

This article continues the effort in deriving the force–displacement compliance relations for a system of two particles bound with a binder. The previous work done in this topic (Zhu et al., 1996a,b, 1997b) is the derivation of 3-D contact laws. This article is devoted to the 2-D analysis (plane stress and plane strain). Although the methodology employed in this article is similar to those given in the previous work, this study presents a number of new results. The first one is that the contact compliance now becomes dependent on the size variable of cylindrical particles. This dependence provides a correlation of the volumetric ratio of the binder to particles in the contact compliance with the fiber volume ratio, an important quantity in fibrous composites. As such, the binder compliance can be delegated to its applications in the area of the mechanics of fibrous composites.

Progression of the compliance derivation in this article begins with establishing the integral equations that govern the contact pressure distribution at the interface of the particles and the binder. Two limiting

* Corresponding author. Tel.: +1-602-965-2745; fax: +1-480-965-0557.
E-mail address: han.zhu@asu.edu (H. Zhu).

0020-7683/00/$ - see front matter
PII: S0020-7683(00)00002-0

cases with respect to (1) rigid binder and (2) rigid particles are first pursued in which the exact compliances can be solved analytically. Using those two limiting case solutions to construct the upper and lower bounds then yields the two close-form contact compliances. Two more results of contact compliance are obtained by substituting the pressure unknowns in the integral equations with the appropriate limiting-case solutions. With four groups of contact compliance derived, the final representation of contact compliances is selected on a physically rational basis. Three types of contact compliance are obtained and they are (1) elastic binder, (2) Maxwell binder and (3) Voigt binder. Particles are always assumed to be elastic.

Since the methodology employed in the aforementioned progression basically follows what is given in Zhu et al. (1997a), Zhu (1998, 1999) and Zhu and Nodes (1999), most derivation steps are omitted and only major results are presented.

Most studies on contact compliances make the assumption either explicitly or implicitly that the ratio of the characteristic dimension of the contact area, denoted by a in this article, to that of the contact particles, denoted by H, is infinitesimal. Thus, in the analytical compliance analysis the influence from those terms that are proportional to $(a/H)^n$, $n = 1, 2, 3, \ldots$ on compliance is discarded when the power index n is greater than 1. This is also true in the foregoing 3-D compliance derivation. But this article makes an effort in attempting a more vigorous analysis by using the concept of Taylor series expansion that the term of $(a/H)^2$ is incorporated in the compliance derivation. A compliance comparison for a special case (zero binder thickness) will then be given, which includes the results from this article as well as the other two of the non-Hertzian contact and the Timoshenko's and Goddier's solution.

As stated previously, one objective in pursuing this study is to seek the application of the contact compliance in the area of mechanics of fibrous composites. The type of fibrous composites under consideration is a unidirectional lamina. Assuming the fiber distribution in a lamina is totally random, the effective properties of the lamina is then statistically transversely isotropic (Hashin, 1983) and there are five independent effective elastic moduli (Fig. 1). Many methods have been developed in evaluating those moduli which include engineering estimates, representative volume element (RVE), variational approach, self-consistent scheme, composite cylinder assemblage (CCA), the upper and lower bond analysis, etc. Recently, Zhu et al. (1997b), Zhu (1998, 1999), and Zhu and Nodes (1999) introduced a new approach in which a contact mechanism based material property homogenization is characterized. The two transverse moduli now can be approximated by a function of contact compliances. As the last task in this article, the transverse bulk modulus, one of the two transverse moduli, will be computed and its comparison with those from other methods will also be presented.

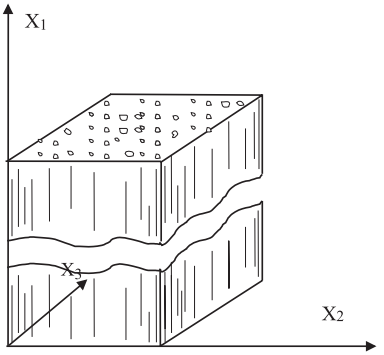

Fig. 1. Unidirectional fiber composite.

2. Formulation of the problem

Fig. 2 shows an axi-symmetric contact configuration in an x–z coordinate in which two half-particles are perfectly bonded by a thin binder. $z = h(x)$ represents the geometry of interfacial boundary between the particles and the binder, and is expressed as

$$h(x) = h_0\left(1 + d\frac{x^2}{a^2}\right), \tag{2.1}$$

where a is the contact arc length, h_0 is the thickness of the binder at $x = 0$, and d, a dimensionless shape parameter related to the curvature of particle surface, is limited in a range $0 \leqslant d < 1$. For a planer surface, d is zero. For a circularly cylindrical particle, d is 1.

We denote the z-displacement field in the particle $w_1(x,z)$, and in the binder $w_2(x,z)$, and the moduli E_p and E_b, Poisson's ratio v_p and v_b for the particles and the binder, respectively (elastic binder). $p(x)$ represents the interfacial normal pressure between the particles and the binder, and P_z is the z-direction resultant force which is related to $p(x)$ by

$$P_z = \int_{-a}^{a} p(x)\,\mathrm{d}x. \tag{2.2}$$

The objective of this study is to seek for the plane stress case how much P_z is, if the plane $z = h_0 + H$ moves downward by an amount of δ_z with the plane $z = 0$ remaining immovable. By definition, the relative normal displacement between $z = 0$ and $z = h_0 + H$ (or the relative approach in the term of contact mechanics) δ_z for the two contact bodies (binder and particle) is given by

$$\delta_z = \delta_{z\mathrm{b}} + \delta_{z\mathrm{p}}, \quad \delta_{z\mathrm{b}} = \int_0^{h(x)} \varepsilon_z(x,z)\,\mathrm{d}z, \qquad \delta_{z\mathrm{p}} = \int_{h(x)}^{h(x)+H} \varepsilon_z(x,z)\,\mathrm{d}z, \tag{2.3}$$

where, ε_z is the strain. $\delta_{z\mathrm{b}}$ and $\delta_{z\mathrm{p}}$ are the relative normal approach contributed by the binder and the particle, respectively.

Since the binder is a thin layer or $h_0/H \ll 1$, we approximate ε_z in the binder to be uniform in the z direction. Then, $\delta_{z\mathrm{b}}$ can be expressed by $w_2(x,z)$ at $z = h(x)$ which follows:

$$\delta_{z\mathrm{b}} = w_2(x, h(x)) = h(x)\frac{p(x)}{E_\mathrm{b}}. \tag{2.4}$$

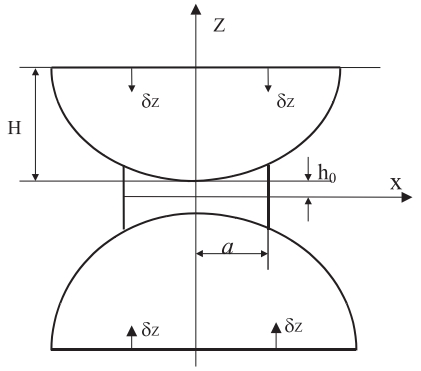

Fig. 2. Sketch of two cylindrical particles bound with a binder.

For the analysis of deformation contribution from the particle, we assume that the characteristic dimension for the particle is much larger than that of the contact area between the particle and the binder, i.e. $a/H \ll 1$, that it is justifiable to pursue the analysis based on a half-space premise. Using the result of Johnson (1985), $\delta_{z\mathrm{p}}$ can be expressed:

$$\delta_{z\mathrm{p}} = \frac{-2}{\pi E_{\mathrm{p}}} \int_{-a}^{a} \ln|x-s|\, p(s)\,\mathrm{d}s + \text{const}, \tag{2.5}$$

and the parameter const is defined as (see Appendix A):

$$\text{const} = \frac{P}{\pi E_{\mathrm{p}}}(2\ln H - 1 - \nu_{\mathrm{p}}). \tag{2.6}$$

Assuming $p(x)$ is an even function of x in $-a < x < a$, and substituting Eqs. (2.4)–(2.6) into Eq. (2.3) yields the $\delta_z - p(x)$ governing equation:

$$\delta_z = \frac{h(x)p(x)}{E_{\mathrm{b}}} + \frac{-2a}{\pi E_{\mathrm{p}}} \int_0^1 \ln|(x/a)^2 - s^2|\, p(as)\,\mathrm{d}s + \frac{P}{\pi E_{\mathrm{p}}}\left(2\ln\frac{H}{a} - 1 - \nu_{\mathrm{p}}\right). \tag{2.7}$$

It can be seen that Eq. (2.7) is a second kind of Fredholm integral equation with a kernel which has a logarithmic singularity. The interfacial pressure function, $p(x)$, can be determined by solving Eq. (2.7).

3. Compliance solutions for elastic binder

3.1. Two limiting cases

The exact solution of the interfacial pressure $p(x)$ in Eq. (2.7) is known for two limiting cases, namely (1) rigid particle case (i.e., $E_{\mathrm{p}} \to \infty$ while E_{b} is finite), and (2) rigid binder case (i.e., E_{p} is finite while $E_{\mathrm{b}} \to \infty$). In the rigid particle case, the relative displacement of the two contact bodies is contributed only from the deformation of binder. Thus $p(x)$ can be easily determined by (denoted as $p_1(x)$):

$$p_1(x) = \frac{E_{\mathrm{b}} C_{z\mathrm{b}} P}{h(x)}, \qquad C_{z\mathrm{b}} = \frac{h_0\sqrt{d}}{2aE_{\mathrm{b}}\,\mathrm{arctg}\,(\sqrt{d})}, \tag{3.1}$$

where d is the shape parameter defined in Eq. (2.1). The corresponding contact compliance is given by

$$\delta_z = C_{z\mathrm{b}} P. \tag{3.2}$$

For the case of rigid binder, using the integral identity:

$$1 = \frac{-2}{\pi \ln 2} \int_0^1 \frac{\ln|x^2 - s^2|}{\sqrt{1-s^2}}\,\mathrm{d}s, \tag{3.3}$$

the exact solution of $p(x)$ is easily determined (Johnson, 1985) (denoted as $p_2(x)$), and it reads

$$p_2(x) = \frac{P}{\pi\sqrt{(a^2 - x^2)}}. \tag{3.4}$$

Substituting $p(x)$ in Eq. (2.7) with $p_2(x)$ in Eq. (3.4) and imposing the condition: $E_{\mathrm{b}} \to \infty$, the compliance relationship for the rigid binder case can be obtained accordingly:

$$\delta_z = C_{z\mathrm{p}} P, \qquad C_{z\mathrm{p}} = \frac{2\ln\left[\frac{2H}{a}\right] - (1+\nu_{\mathrm{p}})}{\pi E_{\mathrm{p}}}. \tag{3.5}$$

3.2. Upper bound compliance solution

Multiplying $1/h(x)$ with Eq. (2.7), and then integrating the equation over the range $0 \leqslant x \leqslant a$, we obtain:

$$\delta_z = C_{zb}P + \frac{2a\sqrt{d}}{\pi E_p \operatorname{arctg}(\sqrt{d})} \int_0^1 f(s,d)p(as)\,\mathrm{d}s + \frac{P}{\pi E_p}\left(2\ln\left[\frac{H}{a}\right] - 1 - \nu_p\right), \tag{3.6}$$

$$f(s,d) = -\int_0^1 \frac{\ln|x^2 - s^2|\,\mathrm{d}x}{1 + \mathrm{d}x^2}. \tag{3.7}$$

Utilizing the monotonic decreasing property of $f(s,d)$ with respect to the variables s and d (Fig. 3), and replacing $f(s,d)$ with 2 since $f(s,d) < f(s=0,d=0) = 2$, the upper bound compliance relation is obtained as:

$$\delta_z < C_{zb}P + C_{zp}b_1P, \tag{3.8}$$

where

$$b_1 = 1 + \frac{\frac{2\sqrt{d}}{\operatorname{arctg}(\sqrt{d})} - 2\ln 2}{\ln\left[\frac{2H}{a}\right] - 1 - \nu_p} > 1. \tag{3.9}$$

3.3. Lower bound compliance solution

Multiplying $p_2(x)$ to Eq. (2.7), and then integrating the equation with respect to the variable s over the range $0 < s < a$, which yields:

$$\delta_z = \frac{4aC_{zb}\operatorname{arctg}(\sqrt{d})}{h_0\sqrt{d}} \int_0^a \frac{p(x)h(x)\,\mathrm{d}x}{\sqrt{a^2 - x^2}} + C_{zp}P. \tag{3.10}$$

It is easily seen that $h(x)(a^2 - x^2)^{-0.5}$ in the integral in Eq. (3.10) increases with respect to x monotonically in the range $0 \leqslant x \leqslant a$, and setting $x = 0$ in $h(x)(a^2 - x^2)^{-0.5}$ in Eq. (3.10) can readily lead to the following inequality:

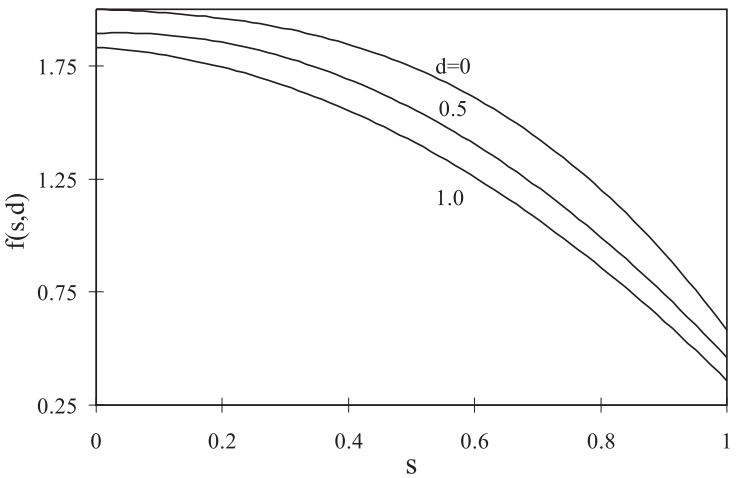

Fig. 3. Monotonic behavior of $f(s,d)$ with respect to s and d.

$$\delta_z > C_{zb} b_2 P + C_{zp} P, \tag{3.11}$$

where

$$b_2 = \frac{2\,\mathrm{arctg}(\sqrt{d})}{\sqrt{d}} < 1, \quad 0 < d < 1. \tag{3.12}$$

Based on the upper and lower bound solutions, the true compliance must meet two following inequalities:

$$b_2 C_{zb} + C_{zp} < \frac{\delta_z}{P} < C_{zb} + b_1 C_{zp}. \tag{3.13}$$

3.4. Two estimates based on physical approximation

The first estimate is pursued by replacing $p(s)$ in the integral in Eq. (3.6) with $p_2(x)$ given in Eq. (3.4) because the integral in Eq. (3.6) represents the deformation contribution from the particle. The compliance relation is

$$\delta_z = (C_{zb} + C_{zp})P. \tag{3.14}$$

The second estimate is pursued by replacing $p(x)$ in the integral in Eq. (3.10) with $p_1(x)$ given in Eq. (3.1) because the integral represents the deformation contribution from the binder. The compliance relation is

$$\delta_z = (C_{zb} + C_{zp})P. \tag{3.15}$$

Based on those four estimates of contact compliance, we thereby select the normal compliance relation given in both Eqs. (3.14) and (3.15) as the best estimate for this particle-binder system:

$$\delta_z = C_z P, \quad C_z = C_{zb} + C_{zp}. \tag{3.16}$$

Eq. (3.16) indicates that the overall compliance corresponds to a serial connection of the two compliances C_{zb} and C_{zp} as schematically shown in Fig. 4a, where C_{zp} represents the particle compliance, and C_{zb} represents that of the binder.

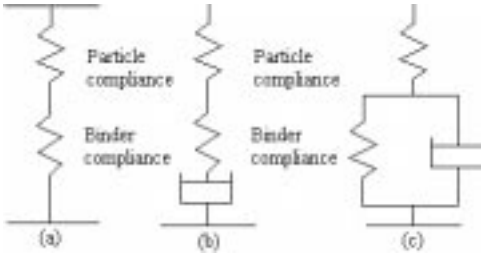

Fig. 4. Equivalent spring-dashpot compliance systems: (a) elastic binder and elastic particle; (b) Maxwell binder and elastic particle; and (c) Voigt binder and elastic particle.

4. Visco-elastic binder

4.1. Maxwell model

The normal stress–strain relationship in the thin layer of Maxwell binder is given by (integral representation):

$$\varepsilon_z(x,t) = \frac{p(x,t)}{E_b} + \frac{1}{\eta}\int_0^t p(x,\tau)\,d\tau, \tag{4.1}$$

where $\varepsilon_z(x,t)$ denotes the normal strain, $p(x,t)$ denotes the normal interfacial stress, and η is the viscosity constant. The governing integral equation in Eq. (2.7) corresponding to the Maxwell binder now becomes

$$\delta_z(t) = h(x)\frac{p(x,t)}{E_b} + \frac{h(x)}{\eta}\int_0^t p(x,\tau)\,d\tau + \frac{-2a}{\pi E_p}\int_0^t \ln\left[(x/a)^2 - s^2\right]p(as,t)\,ds + \frac{P(t)}{\pi E_p}\left(2\ln\left[\frac{H}{a}\right] - 1 - \nu_p\right). \tag{4.2}$$

Again, we attempt to derive an upper bound compliance, a lower bound compliance, and two compliance estimates for the case of Maxwell binder. Since the derivation basically copies what is done in the elastic binder case, only the results are given and they are

$$\text{upper bound} \quad \delta_z(t) \leqslant (C_{zb} + b_1 C_{zp})P(t) + \frac{C_{zb}E_b}{\eta}\int_0^t P(\tau)\,d\tau, \tag{4.3}$$

$$\text{lower bound} \quad \delta_z(t) \geqslant (C_{zb}b_2 + C_{zp})P(t) + C_{zb}b_2\frac{E_b}{\eta}\int_0^t P(\tau)\,d\tau, \tag{4.4}$$

$$\text{two estimates} \quad \delta_z(t) = (C_{zb} + C_{zp})P(t) + C_{zb}\frac{E_b}{\eta}\int_0^t P(\tau)\,d\tau, \tag{4.5}$$

where b_1 and b_2 are defined in Eqs. (3.9) and (3.12), respectively. We select the compliance relation given in Eq. (4.5) as the best estimate for the case of Maxwell binder. Its rate-dependent form is

$$\dot{\delta}_z(t) = (C_{zb} + C_{zp})\dot{P}(t) + C_{zb}\frac{E_b}{\eta}P(t), \tag{4.6}$$

where the symbol "." denotes the derivative with respect to time.

4.2. Voigt model

The stress–strain relationship in its integral representation for the Voigt binder is given by

$$\varepsilon_z(x,t) = \int_0^t \frac{p(x,\tau)}{\eta}\exp\left(-\frac{E_b}{\eta}(t-\tau)\right)d\tau. \tag{4.7}$$

Accordingly, the governing integral equation is

$$\delta_z(t) = \frac{h(x)}{\eta}\int_0^t p(x,\tau)\exp\left(-\frac{E_b}{\eta}(t-\tau)\right)d\tau + \frac{-2a}{\pi E_p}\int_0^t \ln\left[(x/a)^2 - s^2\right]p(as,t)\,ds + \frac{P(t)}{\pi E_p}\left(2\ln\left[\frac{H}{a}\right] - 1 - \nu_p\right). \tag{4.8}$$

Again, the derivation procedure is omitted and the final results are listed:

$$\text{upper bound} \quad \delta_z(t) \leqslant b_1 C_{zp} P(t) + C_{zb} \frac{E_b}{\eta} \int_0^t p(\tau) \exp\left(-\frac{E_b}{\eta}(t-\tau) \right) d\tau, \tag{4.9}$$

$$\text{lower bound} \quad \delta_z(t) \geqslant C_{zp} P(t) + b_2 C_{zb} \frac{E_b}{\eta} \int_0^t p(\tau) \exp\left(-\frac{E_b}{\eta}(t-\tau) \right) d\tau, \tag{4.10}$$

$$\text{two estimates} \quad \delta_z(t) = C_{zp} P(t) + C_{zb} \frac{E_b}{\eta} \int_0^t P(\tau) \exp\left(-\frac{E_b}{\eta}(t-\tau) \right) d\tau \tag{4.11}$$

We select the compliance relation given in Eq. (4.11) as the best estimate for the case of Voigt binder, and its rate-dependent version is

$$\delta_z(t) + \frac{E_b}{\eta} \delta_z(t) = C_{zb} \dot{P}(t) + (C_{zb} + C_{zp}) \frac{E_b}{\eta} P(t). \tag{4.12}$$

Fig. 4b and c depict two spring-dashpot systems that represent equivalently Eq. (4.6) for the Maxwell binder and Eq. (4.12) for the Voigt binder, respectively.

5. Analysis of finite (a/H) ratio

Deriving the contact compliances given in the above so far takes the assumption that $a/H \ll 1$. This assumption is reflected in Eqs. (2.5) and (2.6) that the parameter const is a constant determined in Eq. (A.1) in which the integral in the right-hand side of Eq. (A.1) is first expanded into a Taylor series of $(a/H)^n$, $n = 0, 1, 2, \ldots$ and then the truncation is made to those terms $(a/H)^n$ with the power index n being greater than zero. To pursue a more vigorous analysis, the parameter const needs to include higher orders of a/H. For this purpose, Eq. (A.1) is modified to include the terms of (a/H) and $(a/H)^2$ and the parameter const now is a function of x and reads

$$\text{const} = \frac{P(2\ln H - 1 - \nu_p)}{\pi E_p} + \frac{2+\nu_p}{\pi H^2 E_p} \int_{-a}^{a} (x-s)^2 p(s)\, ds. \tag{5.1}$$

Replacing const in Eq. (2.5) with the above expression yields the contact governing equation for the elastic binder which contains the term of $(a/H)^2$:

$$\delta_z = \frac{h(x)p(x)}{E_b} + \frac{-2a}{\pi E_p} \int_0^1 \ln\left[(x/a)^2 - s^2\right] p(as)\, ds + \frac{(2+\nu_p)x^2 P}{\pi H^2 E_p} + \frac{P}{\pi E_p}\left(2\ln\left[\frac{H}{a}\right] - 1 - \nu_p \right) + \frac{2(2+\nu_p)a^3}{\pi H^2 E_p} \int_0^1 s^2 p(as)\, ds. \tag{5.2}$$

Eq. (5.2) is again a second kind of Fredholm integral equation with a kernel which has a logarithmic singularity and a free term having both a constant and x^2. A similar compliance derivation will be conducted here. The first step is to derive the limiting case of rigid binder by letting E_b in Eq. (5.2) approach to infinite, and the governing equation for the rigid binder case is

$$\delta_z = \frac{-2a}{\pi E_p} \int_0^1 \ln\left[(x/a)^2 - s^2\right] p_2(as)\, ds + \frac{(2+\nu_p)x^2 P}{\pi H^2 E_p} + \frac{P}{\pi E_p}\left(2\ln\left[\frac{H}{a}\right] - 1 - \nu_p \right) + \frac{2(2+\nu_p)a^3}{\pi H^2 E_p} \int_0^1 s^2 p_2(as)\, ds, \tag{5.3}$$

where, $p_2(x)$ is again denoted as the pressure variable for the rigid binder case. The force balance condition is

$$P = a\int_{-1}^{1} p_2(as)\,\mathrm{d}s. \tag{5.4}$$

The exact solution for $p_2(x)$ is also available. Baker (1978) proved the following integral identity:

$$\int_{-1}^{1} \ln|(x/a)-s|\sqrt{1-s^2}\,\mathrm{d}s = -\left(\frac{\pi}{4}+\frac{\pi}{2\ln 2}\right)+\frac{\pi}{2}\frac{x^2}{a^2}, \quad -a\leqslant x\leqslant a. \tag{5.5}$$

Based on both Eqs. (3.3) and (5.5), $p_2(x)$ can be composed as:

$$p_2(x) = \frac{q_1 P}{\sqrt{a^2-x^2}}+\frac{q_2 P}{a^2}\sqrt{a^2-x^2}, \tag{5.6}$$

where q_1 and q_2 are two undetermined dimensionless constants. By carrying out the integration in Eq. (5.4) (force balance) with $p_2(x)$ being defined in Eq. (5.6), one linear equation with respect to q_1 and q_2 is obtained:

$$1 = q_1\pi + 0.5q_2\pi. \tag{5.7}$$

Also, by implementing the integration in Eq. (5.3), with $p_2(x)$ being defined in Eq. (5.6), the following identity is obtained:

$$(\delta_z - C^*_{z\mathrm{p}}P)+P\left(q_2-\frac{(2+\nu_\mathrm{p})a^2}{\pi H^2}\right)x^2 = 0, \tag{5.8}$$

$$C^*_{z\mathrm{p}} = C_{z\mathrm{p}} - \frac{2q_2\ln 2}{E_\mathrm{p}}. \tag{5.9}$$

Consolidating Eqs. (5.7)–(5.9) yields the following results:

$$q_1 = \frac{1}{\pi} - 0.5q_2, \tag{5.10}$$

$$q_2 = \frac{(2+\nu_\mathrm{p})a^2}{\pi H^2}, \tag{5.11}$$

and the compliance relation for the rigid binder case is now

$$\delta_z = C^*_{z\mathrm{p}}P \tag{5.12}$$

$$C^*_{z\mathrm{p}} = C_{z\mathrm{p}} - \frac{2\ln 2(2+\nu_\mathrm{p})a^2}{\pi H^2 E_\mathrm{p}}. \tag{5.13}$$

Regarding the rigid particle case, it can be easily seen that when setting $E_\mathrm{p}\to\infty$ in Eq. (5.2), $p_1(x)$ defined in Eq. (3.1) is still a valid solution. Thus, the compliance relation for the rigid particle case remains unchanged for both infinitesimal and finite (a/H) ratios.

The subsequent analysis on the upper and lower bounds, and two estimates on the physical approximation is an almost repeating process referring to what is done in Section 3. The conclusion is that all the results from the previous section remain valid for the current study of finite (a/H) ratio after replacing $C_{z\mathrm{p}}$ in Eq. (3.5) with $C^*_{z\mathrm{p}}$ in Eq. (5.13). For the elastic binder case, the compliance relation is

$$\delta_z = (C_{z\mathrm{b}} + C^*_{z\mathrm{p}})P. \tag{5.14}$$

The same conclusion is also true for the case of Maxwell and Voigt binder. All the results from Section 4 remain valid after replacing C_{zp} in Eq. (3.5) with C^*_{zp} in Eq. (5.13).

6. Complaince comparison

The case under study in this section is a system of two particles bound with a binder. One limiting case of this system is that when the binder disappears and two particles come into contact. The particle compliance derived from the current analysis is represented by C_{zp} in Eq. (3.5) and C^*_{zp} in Eq. (5.13). This is also the case in which two previous studies were done; one is called the non-Hertzian contact (Johnson, 1985), and the other can be found in the book of Timoshenko and Goddier (1951). In this section, those four compliances are first normalized (CN) and listed as follows:

$$\begin{aligned}
\mathrm{CN} &= \frac{\pi E_p C_{zp}}{(1-\nu_p^2)2\ln\left[\frac{2H}{a}\right]} = 1 - \frac{\nu_p}{(1-\nu_p)2\ln\left[\frac{2H}{a}\right]} \quad (\textit{non-Hertzian contact}),\\
&= 1 + \frac{2\ln 2 - 1}{2\ln\left[\frac{2H}{a}\right]} \quad (\textit{Timoshenko, Goddier}),\\
&= 1 - \frac{1}{(1-\nu_p)2\ln\left[\frac{2H}{a}\right]} \quad (\textit{current}, a/H \ll 1),\\
&= 1 - \frac{\frac{1}{1-\nu_p} + \frac{2\ln 2(2-\nu_p)a^2}{(1-\nu_p)H^2}}{2\ln\left[\frac{2H}{a}\right]}, (\textit{current, finite } a/H).
\end{aligned} \tag{6.1}$$

By setting $\nu_p = 0.25$, all four normalized compliances in Eq. (6.1) are computed and plotted in Fig. 5 versus a/H. The curves in Fig. 5 show that when a/H is near zero, all four compliances approaches 1. But finite values of a/H do make a difference to the compliances. Fig. 5 also shows that the finite a/H ratio effect on compliance is the increase in the contact stiffness. This stiffness increase is physically correct because now a finite region, not a half infinite space as assumed in the derivation of other three compliances, contributes the accumulation of the deformation to δ_z.

7. Transverse bulk modulus

Following the notation used by Hashin (1983), the stress–strain equations for a unidirectional fibrous composite sketched in Fig. 1 and for the plane strain case ($\varepsilon_{11} = 0$) may be written as:

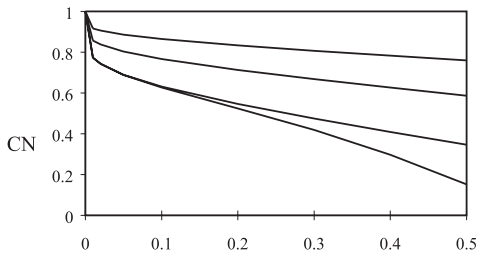

Fig. 5. CN versus a/H. From top to bottom: non-Hertzian contact, Timoshenko and Goddier, current result with $a/H \ll 1$, and current result with finite a/H.

$$\begin{aligned}\sigma_{22} &= (k^* + G_T^*)\varepsilon_{22} + (k^* - G_T^*)\varepsilon_{33},\\ \sigma_{33} &= (k^* - G_T^*)\varepsilon_{22} + (k^* + G_T^*)\varepsilon_{33},\end{aligned} \tag{7.1}$$

where, σ_{22}, σ_{33} are the effective stresses, ε_{22} and ε_{33} are the effective strains. k^* and G_{T}^* are called transverse bulk modulus and transverse shear modulus, respectively. Here the distribution of fibers is assumed to be totally random. The study of the upper and lower bounds for k^* were conducted by Hashin (1983)and Hill (1964) and they are expressed as:

$$\text{lower bound} \quad k^*(\text{lower}) = k_1 + \frac{V_2}{1/(k_2 - k_1) + V_1/(k_1 + G_1)}, \tag{7.2}$$

$$\text{upper bound} \quad k^*(\text{upper}) = k_2 + \frac{V_1}{1/(k_1 - k_2) + V_2/(k_2 + G_2)}, \tag{7.3}$$

where V_1, G_1 and k_1 denote the volume ratio, shear modulus and transverse bulk modulus for the matrix, respectively. V_2, G_2 and k_2 denote the volume ratio, shear modulus and transverse bulk modulus for fibers, respectively.

Zhu et al. (1997a) introduced a contact mechanism based analysis of effective property for fibrous composites. The stress–strain equations corresponding to Eq. (7.1) are

$$\begin{aligned}\sigma_{22} &= \left(\frac{5\sqrt{3}K_{\mathrm{n}}}{8} + \frac{\sqrt{3}K_{\mathrm{s}}}{5}\right)\varepsilon_{22} + \left(\frac{5K_{\mathrm{n}}}{8\sqrt{3}} - \frac{\sqrt{3}K_{\mathrm{s}}}{5}\right)\varepsilon_{33},\\ \sigma_{33} &= \left(\frac{5K_{\mathrm{n}}}{8\sqrt{3}} - \frac{\sqrt{3}K_{\mathrm{s}}}{5}\right)\varepsilon_{22} + \left(\frac{5\sqrt{3}K_{\mathrm{n}}}{8} + \frac{\sqrt{3}K_{\mathrm{s}}}{5}\right)\varepsilon_{33},\end{aligned} \tag{7.4}$$

where, K_{n} and K_{s} are the normal and tangential contact stiffness coefficients, respectively. Observing Eqs. (7.1) and (7.4) easily reveals

$$k^* = \frac{5K_{\mathrm{n}}}{2\sqrt{3}} = \frac{5}{4\sqrt{3}(C_{z\mathrm{b}} + C_{z\mathrm{p}}^*)}, \tag{7.5}$$

where, K_{n}, by definition, is inversely proportional to half of the compliance given in Eq. (5.14).

The compliance representation given in Eq. (5.14) is derived for the plane stress case. Replacing ν_{p} with $\nu_{\mathrm{p}}/(1-\nu_{\mathrm{p}})$, $1/E_{\mathrm{p}}$ with $(1-\nu_{\mathrm{p}}^2)/E_{\mathrm{p}}$ and $1/E_{\mathrm{b}}$ with $(1-\nu_{\mathrm{b}}^2)/E_{\mathrm{b}}$ in the derivation gives rise to the compliance result for the plane strain case. Thus, now we can compute k^* for the plane strain case, and compare it with the upper and lower bounds expressed in Eqs. (7.2) and (7.3).

Fig. 6 shows the values of k^* determined by three methods: the upper bound, defined in Eq. (7.2); the lower bound defined in Eq. (7.3) and the contact based evaluation defined in Eq. (7.5). Those k^* values vary depending on the ratio of Young's modulus for fibers to that of the matrix for four levels of fiber ratio: $V_2 = 0.4$, 0.5, 0.6 and 0.7. It can be seen that the contact based k^* falls between the upper and lower bounds.

8. Summary

This article presents a study of the force–displacement interaction of two cylindrical particles bound with a binder. The objective is to derive a close-form representation for the contact compliance. The effort made in this article is succeeded in this regard. Three simple compliance results are arrived for elastic binder, Maxwell binder and Voigt binder. Although the results are presented for the plane stress case, replacing ν_{p}

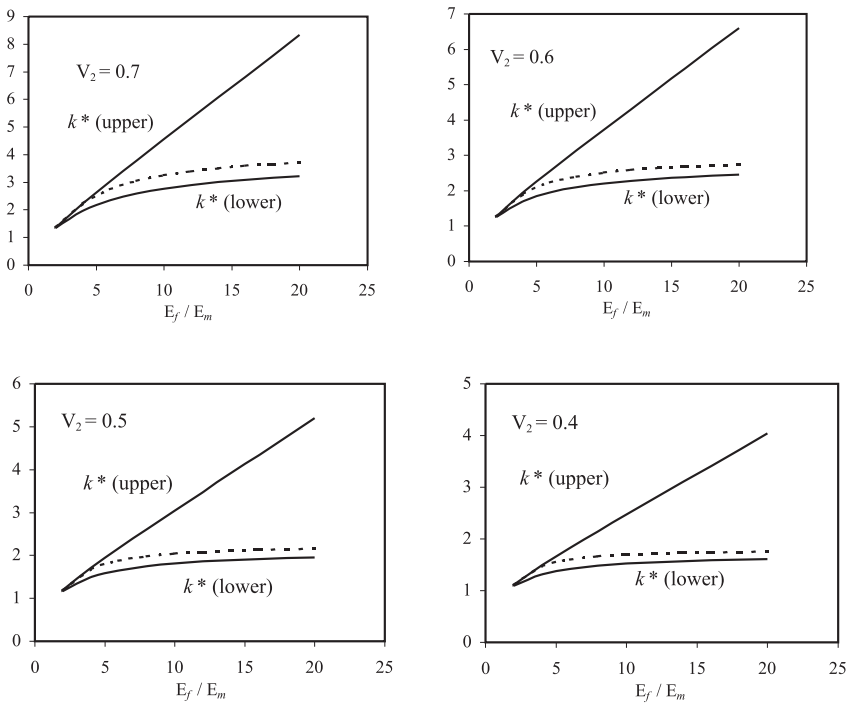

Fig. 6. Comparison of three values of transverse bulk modulus versus the ratio of E_f (Young's Modulus of fibers) to E_m (Young's modulus of the matrix). V_2 is the fiber volume ratio. Dashed lines represent the contact result defined in Eq. (6.5).

with $v_p/(1-v_p)$, $1/E_p$ with $(1-v_p^2)/E_p$ and $1/E_b$ with $(1-v_b^2)/E_b$ in derived compliances yields the solution for the plane strain case.

Another major work of this article is to include the analysis on the effect of finite ratio for a/H on compliances. This inclusion is important because one of the applications for deriving contact compliances aims at the area of the mechanics of fibrous composites. Eliminating the condition of infinitesimal a/H in the compliance derivation makes the connection of how to apply the result obtained in this article to their application in composite materials.

As an example of the compliance application in evaluating effective properties of an unidirectional fiber composite, one of the moduli, k^* (transverse bulk modulus), is computed based on a contact mechanism homogenization analysis and the contact compliances derived in this article. The results are presented in Fig. 6 for the fiber volume ratio being 0.4, 0.5, 0.6 and 0.7. These four ratios are chosen because they cover mostly possible fiber concentrations in typical engineering fibrous composites. The same k^* quantity (lower bound) can also be obtained by using the method of composite cylinder assemblage (CCA). CCA is a method founded on the continuum concept. On the other hand, the contact method characterizes a discrete approach. These two methods are very different in that respect, but they share one thing that, simplistically speaking, they follow in principle so called the iso-stress model that the physical element of fibers and the matrix is arranged in a series connection (Fig. 7a). Both methods give the values of k^* that are not very apart. Calculation of the upper bound for k^* is based on the model of iso-strain in which the physical element of fibers and the matrix is arranged in a parallel connection (Fig. 7b). As such, when Young's modulus for fibers becomes very big in comparison with that of the matrix, k^* computed by CCA and the contact method becomes dominantly dependent on Young's modulus for the matrix, while the upper bound for k^* shows to be proportional to Young's modulus for fibers.

Fig. 7. (a) Iso-stress model, (b) iso-strain model.

The Section 7 presents an analysis of how to pursue the binder compliance based evaluation of transverse bulk modulus, and its results are given in Fig. 6. The evaluation of other effective modulus components is also under pursuing. It appears that one important advantage of the contact mechanism based analysis in the area of mechanics of composite materials is that the viscous nature of matrix materials can be both analytically and quantitatively incorporated into the constitutive analysis by a physics based delegation course. Most matrix materials in engineering composites show a viscous nature, and asphalt pavement is one of them. One important application of the contact compliance for the Maxwell binder case is in the simulation of asphalt pavement. Recently, a cylindrical creep model based on the contact mechanism is developed in simulating laboratory creep tests on asphalt pavement, in which the Maxwell contact compliance is incorporated. More details can be found in the work by Zhu (1999), Zhu and Nodes (1999).

Acknowledgements

Special thanks to the reviewer for his comments on a number of critical issues upon which the revision of the manuscript is mainly made.

Appendix A

The parameter const is defined as a value of an indefinite integral at $z = H$, which reads (plane stress):

$$\text{const} = \frac{1}{E_\text{p}} \int [\sigma_z(x,z) - \nu_\text{p}\sigma_x(x,z)]\,\mathrm{d}z|_{z=H}, \tag{A.1}$$

where

$$\sigma_z = \frac{-2z^3}{\pi} \int_{-a}^{a} \frac{p(s)\,\mathrm{d}s}{[(x-s)^2 + z^2]^2},$$
$$\sigma_x = \frac{-2z}{\pi} \int_{-a}^{a} \frac{p(s)(s-x)^2\mathrm{d}s}{[(s-x)^2 + z^2]^2}. \tag{A.2}$$

Imposing $a/H \ll 1$ and spelling out Eqs. (A.1) and (A.2) gives:

$$\text{const} = \frac{-1}{\pi E_\text{p}} \int_{-a}^{a} \left[\frac{H^2}{(x-s)^2 + H^2} - \ln\left((x-s)^2 + H^2\right) \right] p(s)\,\mathrm{d}s - \frac{\nu_\text{p} P}{\pi E_\text{p}} + \frac{\nu_\text{p}}{\pi E_\text{p}} \int_{-a}^{a} \frac{(s-x)^2 p(s)\,\mathrm{d}s}{(x-s)^2 + H^2}$$
$$= \frac{P(2\ln H - 1 - \nu_\text{p})}{\pi E_\text{p}}, \quad a/H \ll 1. \tag{A.3}$$

References

Baker, C.T.H., 1978. The Numerical Treatment of Integral Equations. Clarendon Press, Oxford.

Hashin, Z., 1983. Analysis of composite materials – a survey. J. Appl. Mech. 50, 481–505.

Hill, R., 1964. Theory of mechanic properties of fiber strengthened materials-1 elastic behavior. J. Mech. Phys. Solids 12, 199–212.

Johnson, K.L., 1985. Contact Mechanics. Cambridge University Press, Cambridge, MA.

Timoshenko, S., Goddier, J.N., 1951. Theory of Elasticity. Third ed. McGraw-Hill, New York.

Zhu, H., Chang, C.S., Rish III, J.W., 1996a. Normal and tangential compliance for conforming binder contact. I: elastic binder. Int. J. Solids Struct. 33, 4337–4349.

Zhu, H., Chang, C.S., Rish III, J.W., 1996b. Normal and tangential compliance for conforming binder contact. II: visco-elastic binder. Int. J. Solids Struct. 33, 4351–4363.

Zhu, H., Rish III, J.W., Dass, W.C., 1997a. A constitutive study of two-phase particulate materials. I: elastic binder. Comput. Geotech. 20 (3), 303–323.

Zhu, H., Chang, C.S., Rish III, J.W., 1997b. Rolling compliance for elastic and visco-elastic conforming binder contact. Int. J. Solids Struct. 34, 4073–4086.

Zhu, H., 1998. Contact mechanism based asphalt concrete modeling. Presented in the 12th Engineering Mechanics Conference. San Diego, CA.

Zhu, H., 1999. Cylindrical modeling of a Maxwell matrix composite. In: David, H. (Ed.), Proceedings of the Sixth International Conference on Composites Engineering. Orlando, FL.

Zhu, H., Nodes, J.E., 1999. Contact based analysis of asphalt pavement with the effect of aggregate angularity. Mech. Mater., in press.